JOURNAL OF GEOPHYSICAL RESEARCH, VOL. 97, NO. A4, PAGES 4027–4039, APRIL 1, 1992

Bursty Bulk Flows in the Inner Central Plasma Sheet

V. ANGELOPOULOS,[1,2] W. BAUMJOHANN,[3] C. F. KENNEL,[1,2] F. V. CORONITI,[1] M. G. KIVELSON,[2] R. PELLAT,[1] R. J. WALKER,[2] H. LÜHR[4] AND G. PASCHMANN[3]

High-speed flows in the inner central plasma sheet (first reported by Baumjohann et al. (1990)) are studied, together with the concurrent behavior of the plasma and magnetic field, by using AMPTE/IRM data from $\approx$ 9 to 19 R_E in the Earth's magnetotail. The conclusions drawn from the detailed analysis of a representative event are reinforced by a superposed epoch analysis applied on 2 years of data. The high-speed flows organize themselves in 10-min time scale flow enhancements which we call bursty bulk flow (BBF) events. Both temporal and spatial effects are responsible for their bursty nature. The flow velocity exhibits peaks of very large amplitude with a characteristic time scale of the order of a minute, which are usually associated with magnetic field dipolarizations and ion temperature increases. The BBFs represent intervals of enhanced earthward convection and energy transport per unit area in the y-z GSM direction of the order of 5×10^{19} ergs/R_E^2.

INTRODUCTION

That the flow in the Earth's plasma sheet can be bursty in quiet as well as disturbed times has been pointed out in the past [*Coroniti et al.*, 1978,1980]. However, most attention has focused on plasma sheet variability during large magnetospheric substorms. The prominence of boundary layer flows during such intervals [*DeCoster and Frank*, 1979; *Forbes et al.*, 1981] and the recognition that the plasma sheet boundary layer (PSBL) is a permanently active region of the magnetotail [*Lui et al.*, 1983; *Eastman et al.*, 1984, 1985] directed attention away from the dynamics of the central plasma sheet (CPS).

Individual case studies have, at times, pointed out the existence of high-speed CPS flows during active magnetospheric conditions and discussed their consequences [e.g., *Huang et al.*, 1987; *Sergeev et al.*, 1990]. In particular, *Sergeev et al.* [1990] analyzed two time intervals of steady magnetospheric convection, usually attributable to conditions of prolonged, southward pointing interplanetary magnetic field (see, e.g., *Pytte et al.* [1978]). By inferring the plasma sheet bulk velocity from the measured magnetic and electric field on board the ISEE 1 satellite they identified intervals when pulses of earthward directed convection enhancements occurred. These had amplitudes of the order of 250 km/s, a characteristic time scale of a few minutes, and were accompanied by increases of both the magnetic field in the z_{GSM} direction and the total magnetic field magnitude. The bursts were detected at a downtail distance of x_{GSM} of about 17 R_E and were argued to have an (inferred) scale size of 15 R_E in the y_{GSM} direction and fast shock properties.

Statistical studies have also been used to characterize plasma sheet flows. Prior to 1986 only a few of these studies addressed plasma sheet flows irrespective of substorm phase [*Caan et al.*, 1979; *Hayakawa et al.*, 1982; *Slavin et al.* 1985, 1987]. For example, *Hayakawa et al.* [1982] using IMP 6 data from distances of $-15\ R_E < X_{GSM} < -33\ R_E$ showed that high-speed flows (V_x > 300 km/s) can occur in the plasma sheet within 1 R_E from the expected neutral sheet position defined by the *Russell and Brody* [1967] model, so one might infer that these flows occurred in the CPS. However, the above statistical studies either did not distinguish between the CPS and its boundary or they concentrated in the distant-tail regions [*Slavin et al.*, 1985, 1987].

The first statistical assessment of the significance of the near-Earth CPS for magnetotail transport was made by *Huang and Frank* [1986]. They constructed a data base using 128-512 s resolution plasma data from the ISEE 1 satellite. They applied the criterion that high-speed flows (V_i > 150 km/s) occurring 1.5 R_E or more away from the GSM equatorial plane are in the PSBL. They found that the average speed in the CPS was low (around 50 km/s) regardless of geomagnetic activity (based on the *AE* index). They showed (see also Figure 2 of *Huang and Frank* [1987]) that even if high-speed flows existed in their data set, these were not representative of the average properties of the CPS. They therefore argued that even if high-speed flows of short time or spatial scales may occur in the CPS, they are statistically insignificant compared to the vast majority of the (low flow velocity) data. The above study did not attempt to assess the relative contributions of the CPS and the plasma sheet boundary to magnetotail transport.

A new statistical selection criterion to distinguish between the central plasma sheet and its boundary was proposed by *Baumjohann et al.* [1988] (subsequently referred to as BJetal88): the imbalance between the measured electron and ion densities at the lobeward edges of the plasma sheet. This is usually interpreted as an enhancement of photoelectron counts in the low-density and low-temperature plasma sheet boundary plasma [e.g., *Pedersen et al.*, 1985]. BJetal88 showed that this imbalance can reliably separate the PSBL from the CPS samples, in a statistical sense.

BJetal88 surveyed the plasma properties of the PSBL using high time resolution (4.5 s) data from the three-dimensional (3D) plasma instrument on board the AMPTE/IRM satellite. Their study revealed that low-velocity flows dominate the

[1]Department of Physics, University of California, Los Angeles.
[2]Institute of Geophysics and Planetary Physics and Department of Earth and Space Sciences, University of California, Los Angeles.
[3]Max-Planck-Institut für extraterrestrische Physik, Garching, Germany.
[4]Institut für Meteorologie der Technischen Universität Braunschweig, Braunschweig, Germany.

Paper number 91JA02701.
0148-0227/92/91JA-02701 $05.00

statistical distribution of boundary layer samples. As a result, under all geomagnetic conditions the average velocity in the PSBL was low. In fact, the average velocity in the PSBL was shown to be as small as that at the CPS, based on the statistical analyses of *Huang and Frank* [1986, 1987] (compare Figure 1 of Huang and Frank with Figure 8 of BJetal88). It is noteworthy (see Figure 9 of BJetal88) that flows above 300 km/s are observed only 5% of the time for active times (AE > 500 nT), whereas their occurrence rate drops to 1–2% for moderate or quiet times (AE < 500 nT). Furthermore, the PSBL flows were shown (in a statistical hence) to be bursty, with a typical duration of only a few tens of seconds: Only a few (3%) of all high speed flows (therein defined as V_i > 300 km/s) remain above the 300-km/s threshold for more than 2 min.

The above findings pertaining to the dynamics of the PSBL quantified the importance of short-lived, high-speed flows for a magnetotail region that was thought to be permanently active. Moreover, they motivated an application of a similar, statistical approach to the investigation of the characteristics of the CPS. *Baumjohann et al.* [1989] (subsequently referred to as BJetal89) undertook this investigation and used the same data set and similar data selection criteria as BJetal88 to identify CPS samples. Their analysis revealed that short time scale high-speed flows do indeed occur at the CPS with a probability of occurrence comparable to that of the PSBL flows. Furthermore, it quantified important aspects of the statistical properties of the CPS ion flows that were not shown in earlier work [e.g. *Huang and Frank*, 1986, 1987].

In particular, BJetal89 showed (see their Figure 5) that flows above 300 km/s occur in the CPS 2–3% of the time for active (AE > 500 nT) times and 0.7–0.8% of the time for moderate to quiet times (AE < 500 nT). These high-speed flows most often last less than 1 min (fewer than 3% of them remain above the 300-km/s threshold for more than 100 s), they are separated by longer periods of nearly stagnant plasma, and they are directed predominantly earthward.

The high-speed flows in the CPS share, qualitatively, many of their statistical characteristics with the flows at the boundary layer, described previously by BJetal88. However, BJetal89 pointed out that the CPS velocity is typically representative of the bulk flow of a single-ion component rather than the imbalance between two counterstreaming ion beams, as is often the case in the boundary layer. The validity of the above statement for flows close to the neutral sheet, under a wide range of geomagnetic conditions was assessed in a recent survey of the three-dimensional AMPTE/IRM ion velocity distribution functions by *Nakamura et al.* [1991]. The authors showed that during CPS crossings with magnetic field strength B < 5 nT (defined therein as neutral sheet encounters), ring or other peculiar types of distributions occur only rarely. As the ion distribution functions do not deviate from that of a single-ion population, the bulk velocity is a good measure of the plasma flow characteristics in that region of the magnetotail.

The realization that the CPS can occasionally be as dynamic as its boundary reopened the question of the relative occurrence frequency of the CPS and PSBL high-speed flows. This question could not be answered conclusively by the earlier studies (BJetal88, BJetal89) because of the peculiarities of the 1986 AMPTE/IRM orbits that comprised the available data sets. This issue was addressed by *Baumjohann et al.* [1990] (subsequently referred to as BJetal90), who added the 1985 AMPTE/IRM plasma sheet crossings to their data pool to improve their statistics. More specifically, the authors used plasma moments from the 3D plasma instrument and magnetic field data from the fluxgate magnetometer on board the AMPTE/IRM satellite, at 4.5-s resolution, from tail crossings (within $|Y_{GSM}| < 15\ R_E$ and $X_{GSM} < -9\ R_E$). Lobe samples were excluded using the criterion that the partial densities of 1.8–30 keV electrons and 8.5–40 keV ions should be above the two-count level threshold for a sample to belong to the plasma sheet (PS). PS samples were grouped into CPS and PSBL intervals based on the aforementioned "photoelectron" criterion, implemented such that $N_e > N_i^{0.86}$ defines the PSBL. CPS crossings were further grouped into inner and outer central plasma sheet intervals (ICPS and OCPS, respectively) based on magnetic field criteria: It was required that $B_{xy}=(B_x^2+B_y^2)^{1/2} < 15$ nT or $B_z/B_{xy} > 0.5$ for the sample to belong in the ICPS (a condition subsequently referred to as the "ICPS criterion"). If both the "ICPS" and the "photoelectron" criterion were satisfied, the sample was considered to belong to a low-density inner central plasma sheet.

The BJetal90 study proved that high-speed ion flows (therein defined as V_i > 400 km/s) occur in the CPS almost as frequently as in the PSBL; the occurrence rates in the PSBL, OCPS and ICPS are in the ratio 4:1:2 for flows less than 600 km/s and 1:0:1 for flows above 800 km/s. High-speed flows are most likely to occur close to the midnight meridian and at maximum downtail distances. The majority of the flow events in the plasma sheet do not remain above the (arbitrary) threshold of 400 km/s for more than 10 s. An increase of the velocity threshold from 400 to 700 or 1000 km/s results in an increase of the percentage of flows that last only 5 s from 34% to 40% or 46%, respectively (see their Figure 6), attesting to the bursty nature of the flows in the three PS regions. However, the authors showed that ICPS high-speed flows differ from flows in all other PS regions in that they are predominantly perpendicular to the instantaneous magnetic field. Thus they represent cross-field transport.

The BJetal90 statistical study suggests that the ICPS high-speed flows play an important role in plasma sheet dynamics. It also raises several questions that are difficult to answer by means of a statistical study: Are the ICPS high speed flows isolated bursts of duration less than 10 s or parts of a larger, coherent structure? Is there a consistent magnetic field signature associated with them? How do other plasma characteristics evolve during high-speed flows?

In the present paper we report on the features of the ICPS high-speed flow events that emerge when high-speed flow samples are studied on a case by case basis. We also use the superposed epoch analysis technique to establish some of their properties in a statistical manner. We will see that the flow velocity during the time of occurrence of a high-speed flow event is usually extremely variable, that its magnitude typically possesses peaks of full width at half maximum (FWHM) duration of the order of 1 min and that the peak velocities are much larger than the statistically expected average convection velocity of $V_c(AE) \approx$ 50-100 km/s for the concurrent value of the AE index [BJetal89; *Huang and Frank*, 1986]. We will see that these velocity peaks are embedded in longer, 10-min time scale, enhanced velocity structures, whose intermittent nature may be due to spatial effects (i.e., motion of the spacecraft across an "active" region) or temporal changes (i.e., onset/subsidence of flows). In addition, the velocity

exhibits local peaks on the 5-10 s time scale superposed on its average profile, some of which would have been considered independent events in the statistical analyses cited above.

We will refer to the order of a minute time scale velocity peaks of amplitude an order of magnitude larger than the statistically expected average convection velocity $V_c(AE)$ as flow bursts (FBs). We will not address the shorter time scale variability of the flow velocity. We will term the 10-min time scale enhanced flow events (enhanced above the level of a few times $V_c(AE)$) that envelop the FBs, bursty bulk flow events (BBF events) to stress the fact that, in contrast to boundary layer flows, they represent a bulk (usually convective) flow of a single population.

INDIVIDUAL BURSTY BULK FLOW EVENTS

2.1. *BBF Selection Criteria*

In the analysis described in this section we used 5-s averages of the plasma moments measured by the 3D plasma instrument [*Paschmann et al.*, 1985] and 5-s averages of the magnetic field measured by the fluxgate magnetometer [*Lühr et al.*, 1985] on board the AMPTE/IRM satellite. The plasma moments were calculated on board the spacecraft from measured three-dimensional ion and electron distributions every spin period (4.5 s). In this calculation it was assumed that all ions are protons. The 5-s averages of the plasma moments were calculated by "block averaging" the 4.5-s resolution data, i.e., by binning the data into 5-s universal time bins and then averaging. This means that the 5-s averages were usually based on one spin sample. The ambient magnetic field was sampled 32 times per second with a resolution of 0.1 nT. It was also block averaged to a resolution of 5 s.

We visually inspected data from a subset of the interval used in the statistical analysis of BJetal90. Throughout this paper we adopt the same criteria as BJetal90, described in the introduction, to identify the lobe, PSBL, OCPS, and ICPS regions. (We refer to them as the "BJetal90 selection criteria.") We do this even when analyzing plasma sheet crossings in detail, despite the fact that these criteria were developed for a statistical treatment, in an effort to facilitate comparison with the earlier studies of plasma sheet high-speed flows. Using these criteria, we selected high-speed flow events (V_i > 400 km/s for two samples or more, within 1 min) in the ICPS from all the 1985 passes of AMPTE/IRM through the tail ($|Y_{GSM}| < 15\ R_E$ and $X_{GSM} < -9\ R_E$). We examined the structure of the plasma and the magnetic field around 80% of the selected high-speed flow events. The events that we examined occurred from March 24 to May 20, 1985 (a total of 65 events; these can be reorganized into 49 enhanced velocity intervals separated by 10 min or more of low-velocity plasma, i.e., 49 BBF events). The above data set (March 24 to May 20, 1985) includes most of the "neutral sheet" crossings studied by *Nakamura et al.* [1991] (see their Table 1). We will be referring to distribution functions that they published as an additional source of information regarding some of the BBFs that we analyzed.

Ninety percent of the BBF events that we looked at occurred during "active" magnetospheric conditions (AE > 100 nT). This is in agreement with the statistical results of BJetal88 (see their Figure 9 and associated discussion). We found no particular correlation between these "active" time BBFs and substorm phase. The rest (five events) occurred during intervals of low AE, during which it is difficult to assess the condition of the magnetosphere based on the AE index alone. The AE time series during 8-hour intervals within which the five low-AE, BBF events occurred are shown in Figure 1. The downward pointing arrows indicate the times that these five BBFs were detected on AMPTE/IRM; the two upward pointing arrows mark the times of the detection of two substorm-related BBF events. The letters A-E mark BBF events that will be shown in detail in later figures.

It can be seen that even at times of low-AE, BBF events are still associated with some AE variability. These "quiet" time BBF events may occur at a late recovery/early growth phase of a substorm (Figures 1*a*, 1*b*, 1*c* downward pointing arrows) or during an isolated electrojet activity enhancement that does not correspond to a large- scale substorm (Figure 1*d*).

We have also examined ICPS crossings during which the AE index was low and did not show any variability for an interval of many hours. We have not seen any ICPS high-speed flows during such crossings. An example of the AE time series during an ICPS crossing at a downtail distance of $\approx 14\ R_E$ with no BBF events is shown (for comparison with BBF-related AE time series) at the bottom panel of Figure 1. The bar insert indicates the time during which AMPTE/IRM was in the ICPS according to the BJetal90 selection criteria.

Although each event in our data base exhibits its own individuality, we will closely analyze in this study a single representative event (event A of Figure 1) which illustrates the characteristics of most of them, including complexity. We selected to present this particular event for two reasons: (1) The spacecraft remained within the plasma sheet during the entire event; this will help us determine the temporal profile of the phenomenon less ambiguously. (2) AE activity was low, and therefore the event is not related to a large-scale substorm; this will make it easier for us to draw conclusions about its spatial scale and argue about the generality of the phenomenon of BBFs.

In the remaining part of this section we first present the context of the tail crossing within which the selected BBF event occurred, we describe this event in detail, and we obtain a set of derived quantities useful for any theoretically oriented effort to assess its importance. Underlying our choice of a representative event is the assumption that the BBF events that occurred during "active" times and the ones that occurred during "quiet" times (AE < 100 nT) are similar in most of their properties. We address this question in the last part of this section by presenting data during four more BBF events (events B-E of Figure 1).

2.2. *A Representative BBF Event*

2.2.1. *Description of the context of the ICPS crossing.* A 3-hour overview of the plasma sheet measurements that includes the representative BBF event appears in Figure 2. Shown are the AE index at 1-min resolution and plasma and magnetic field data at 5-s resolution from an outbound, midtail crossing of the magnetotail by AMPTE/IRM, from April 10, 1985, at 2200 UT to April 11, 1985, at 0100 UT. The grey-scale bar below the first panel identifies the regions through which the spacecraft was moving, according to the BJetal90 selection criteria. On the basis of ground magnetograms (R. L. McPherron, private communication, 1990) we determined that a moderate substorm with onset around 2130 UT and a

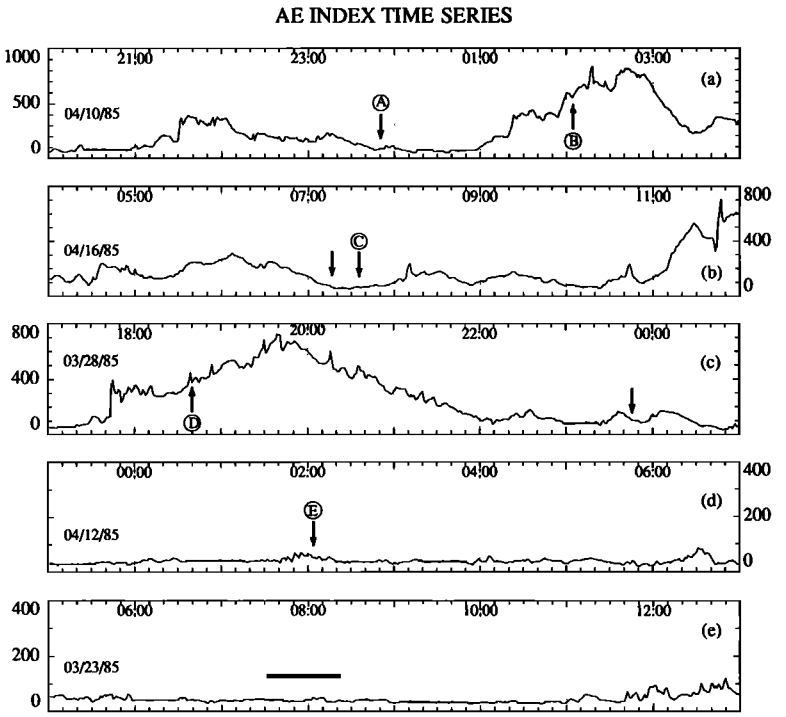

Fig. 1. Five 8-hour time-series of the *AE* index (nanoteslas) around times (indicated by arrows) that BBF events inside the ICPS were detected on the AMPTE/IRM satellite. Notice that the scale is different from panel to panel. Downward pointing arrows indicate times when the five low-*AE* (*AE*<100 nT) BBF events, were detected in the ICPS during the period from March 24 to May 20, 1985. Upward pointing arrows indicate times when two high-*AE* BBF events were detected. (*e*) The *AE* time series for a crossing of the plasma sheet during which no high-speed flows were detected is shown for comparison with (*d*). The bar above the *AE* trace in (*e*) indicates the time during which the spacecraft was in the ICPS at a GSM position of $(X,Y,Z)_{GSM} \approx (-14,1,-1)\ R_E$.

secondary onset around 2315 UT was in its recovery phase but had not fully recovered when it was interrupted by a large substorm with onset around 0120 UT. The 3-hour range K_p index during this event was between 3– and 4 [*Coffey*, 1985], reflecting the moderately disturbed magnetospheric conditions prior to and after the time of the BBF event.

The spacecraft spent most of its time within the PSBL prior to ≈ 2323 UT, at which time it entered the PS and remained there for the rest of the interval shown. Upon entry to the PS, the ion density and temperature continued to increase, as the magnetic field magnitude was decreasing, indicating that the spacecraft was sampling regions closer to the neutral sheet. A factor of 2 decrease in density and an increase in the *B* field at 2333 UT suggest that the spacecraft moved away from the neutral sheet. However, the temperature continued to increase, suggesting that a dynamic process responsible for ion heating may have already started.

The onset of the BBF event is marked by the increase in the velocity magnitude above the average convection level at ≈ 2342 UT. This velocity increase coincided with a sharp decrease in the magnetic field magnitude, which we interpret as a quick entry to the innermost part of the central plasma sheet. The temperature continued to grow even faster until 2346:30 UT (just prior to the peak of the first FB). The level of magnetic field variability increased starting from just prior to the BBF onset and continued throughout the whole time that the spacecraft remained close to the neutral sheet. This is illustrated both by the fluctuations in the magnetic field magnitude in the 5-s resolution data, and by the enhancement in the standard deviation *SB* of the high-resolution magnetic field (32 samples/s) around the 5-s averages. Such an enhancement of the level of the magnetic field fluctuations is characteristic of most of the BBFs that we have inspected.

After about 0005 UT (April 11, 1985) the magnetic field approached the magnitude that it had prior to the onset of the BBF, and its orientation (not shown) resumed its original taillike direction. We interpret this as a passage of the spacecraft to the outermost part of the central plasma sheet. A subsequent series of plasma sheet displacements, evidenced by the fluctuating B_t, brought the neutral sheet closer to the spacecraft several times, but were never accompanied by velocity peaks as large as the ones detected previously. We interpret this as a temporal reduction of the level of the BBF activity. However, the ion velocity did not subside below the statistically expected average convection velocity of $V_c(AE \approx 100$ nT) ≈ 50 km/s for more than an hour.

It is apparent from Figure 2, as it is for all the other ICPS high-speed flow intervals that we have examined, that the flow velocity is large (an order of magnitude larger than $V_c(AE)$) during short intervals of the order of a minute. These we termed flow bursts (FBs). FBs are found within 10-min time scale periods of flow enhancement above the level of a few times $V_c(AE)$, which we termed bursty bulk flow events (BBF events). The flow velocity also possesses structure at time scales shorter than a minute, superposed on an average velocity profile before, during, and after the BBF event. This structure will become clearer in a following, expanded plot.

We chose to focus attention on the 25-min portion of the crossing shown between the vertical lines that includes

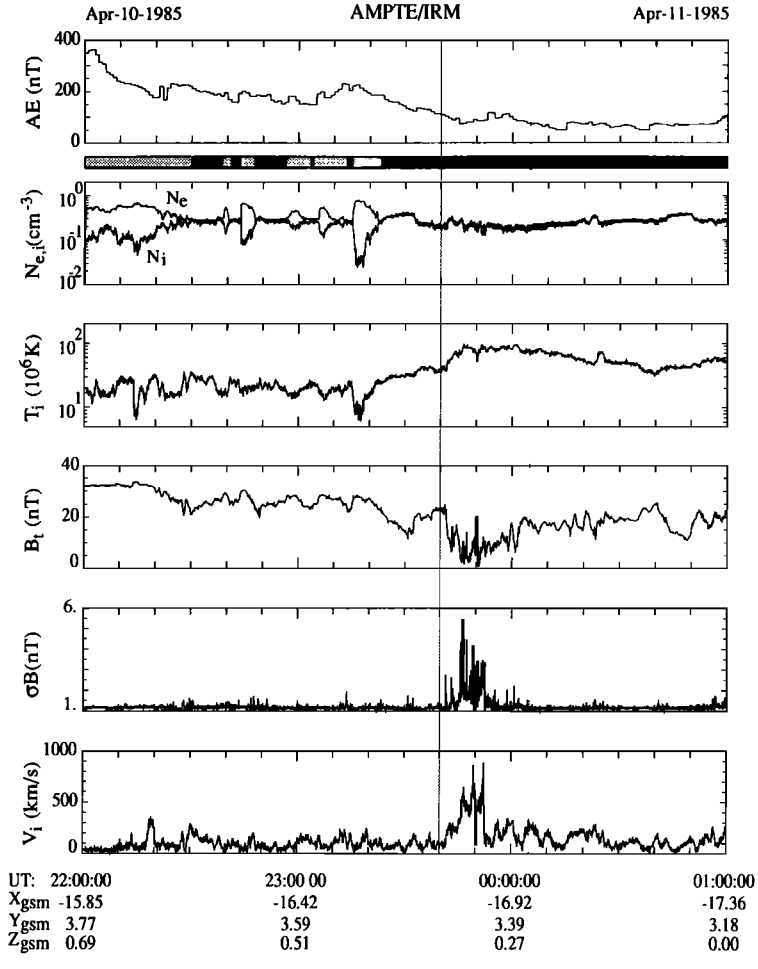

Fig. 2. A 3-hour overview of a plasma sheet, plasma sheet boundary layer encounter during an outbound, midtail crossing of the tail by AMPTE/IRM. The top panel shows the *AE* index at 1-min resolution; the grey-scale bar below it describes the tail region that AMPTE/IRM was traversing (1-min resolution): white corresponds to the lobe, grey to the PSBL and black to the PS. The BJetal90 selection criteria (described in the introduction) were used to identify the different tail regions. The rest of the panels are at 5-s resolution. Shown from top to bottom are: the total electron (N_e, top trace) and proton (N_i bottom trace) densities; the ion temperature T_i; the magnitude of the magnetic field B_t; the standard deviation σB of the full resolution (32 samples/s) magnetic field around its 5-s average (the 1-nT level is due to residual power at the spin period of 4.5-s); the magnitude of the ion bulk speed V_i. Universal time is given at the bottom, as well as the spacecraft location in *X,Y,Z* GSM coordinates. The vertical lines denote the 25-min interval that is expanded in the next figure.

the largest velocity peaks of the BBF event. We believe that the spacecraft was in the ICPS during most (but not all) of this interval. Throughout most of this paper, the magnetic field magnitude and elevation are used to identify the abstract plasma sheet regions (ICPS, OCPS, PSBL) and to serve as spatial indicators of the location of the spacecraft within them, in accordance with the BJetal90 selection criteria. However, we would like to call attention to the fact that with one-satellite data it is not possible to distinguish between plasma sheet oscillations and other temporal changes of the plasma sheet structure (for example, constrictions/dilations). As a result, entry and exit from the different regions of the plasma sheet may in fact reflect a localized, configurational change of a highly dynamic plasma sheet, that bears little relevance to motions of the spacecraft across any persistent, large-scale spatial boundaries. Additional complications may arise from temporal changes of the magnetic field magnitude within individual flux tubes, that are even more difficult to distinguish except for when the spacecraft is very close to the neutral sheet (as will be seen later).

2.2.2. *Overall BBF characteristics.* Figure 3 shows in an expanded format (but still at 5-s resolution) plasma and magnetic field data from the selected 25-min portion of the BBF event. The black shading under the velocity magnitude trace in the top panel emphasizes times when the velocity magnitude exceeded the 400-km/s threshold used in the statistical study of BJetal90. The bar on top of the velocity magnitude panel categorizes the samples (all of which belong to the CPS) into ICPS/OCPS, based on the BJetal90 selection criteria. The magnitude, elevation (θ), and azimuth (ϕ) of the ion velocity and the magnetic field are in the GSM coordinate system.

A sorting of the 5-s samples from this BBF event in a fashion similar to the statistical binning of the 4.5-s samples in the analyses of BJetal89 and BJetal90 would yield characteristics of the plasma sheet high-speed flows reminiscent of those reported in the above studies: The flows are predominantly earthward when their speed is larger than 400 km/s, but they can be arbitrarily oriented when their speed is smaller; the flow speeds are of the order of the local Alfvén velocity,

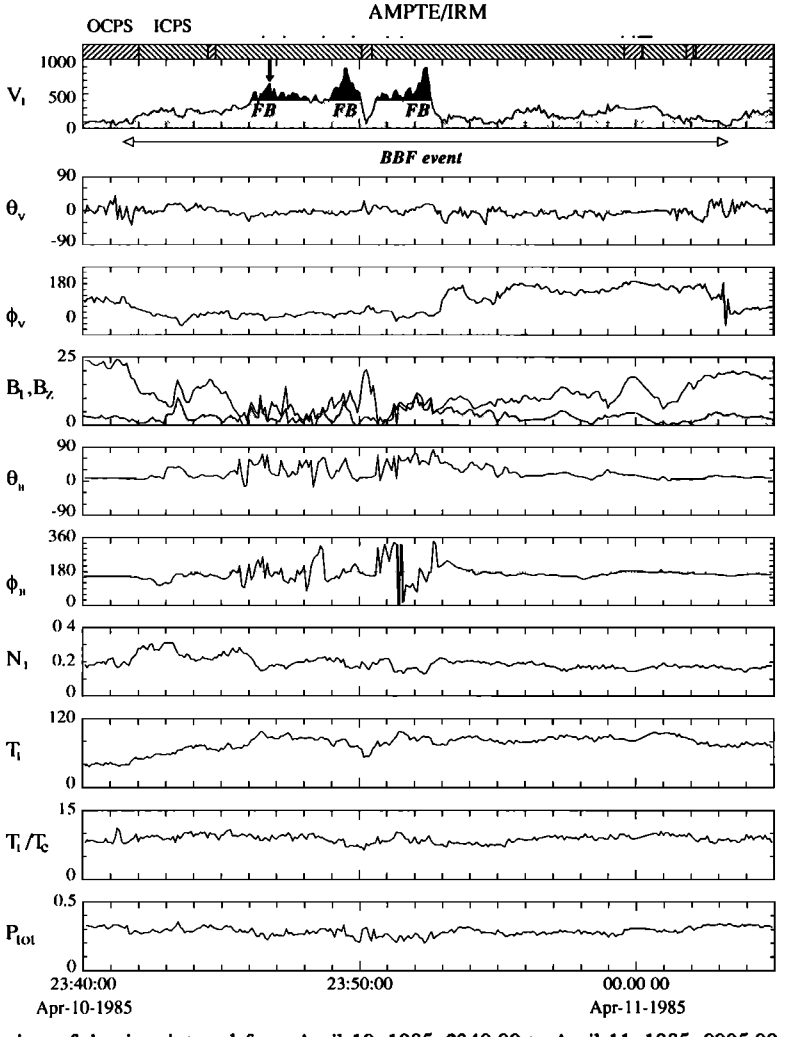

Fig. 3. Expanded view of the time interval from April 10, 1985, 2340:00 to April 11, 1985, 0005:00. All quantities are at 5-s resolution. Vector quantities are in GSM coordinates, in the magnitude, elevation (θ), azimuth (ϕ) format. θ (-90° to 90°) is zero when the vector lies on the xy plane; ϕ (-90° to 270°, mod 360°) is zero when the projection of the vector on the xy plane is pointing sunward, 90° when it is pointing duskward and 180° when it is pointing antisunward. Shown from top to bottom are: the magnitude of the ion bulk velocity V_i (kilometers per second) with grey shading when it was below 400 km/s and black shading when it was above that value; the velocity elevation θ_V; the velocity azimuth ϕ_V; the magnitude of the magnetic field B_t (nanoteslas, top trace) and the z component of the magnetic field B_z (nanoteslas, bottom trace with grey shading); the magnetic field elevation θ_B; the magnetic field azimuth ϕ_B; the ion density N_i (cm^{-3}); the ion temperature T_i (10^6 K); the ion to electron temperature ratio T_i/T_e; the total (sum of magnetic, ion and electron) pressure P_{tot} (nanopascals). Linear interpolation has been applied to remove data gaps. The BBF duration and the positions of the three FBs are marked on the velocity magnitude panel. The bar on top of that panel categorizes the samples (all of which belong to the CPS) into ICPS/OCPS. Samples whose classification would have been inconclusive based on the noninterpolated data are marked with a dot above the ICPS/OCPS indicator bar. The arrow above the first FB points at a time when the ion distribution function was transmitted and published by *Nakamura et al.* [1991] (their Figure 12).

calculated from the instantaneous value of the magnetic field; the flow orientation is often > 45° relative to the occasionally highly dipolar magnetic field. Finally, the speed exhibits local maxima many of which remain above the 400 km/s threshold for no more than 5–10 s, yet there are flows that remain continually above that threshold for a longer time (up to about 2-min). As the threshold is increased from 400 km/s to, for example, 700 km/s the velocity magnitude remains continually above that threshold only for a short time that, eventually approaches the resolution of the plasma instrument. This, as pointed out by BJetal89 and BJetal90, is an indication of the burstiness of the flows.

This case study, which treats the local velocity maxima as parts of the whole BBF event, makes it apparent that the 5-10 s duration local velocity maxima are superposed on a longer time scale velocity profile. The change in the velocity in these more rapid peaks is typically < 200 km/s. In the longer ($\gtrsim$ 1 min), larger profiles the velocity change is $\approx$ 300-600 km/s. We will not be concerned with the shorter, smaller flow bursts in this paper. We can see that this BBF event is composed of a few (three), minute time scale flow velocity peaks of magnitudes ranging from about 500 to 900 km/s (i.e., 10 to 18 times the statistically expected convection velocity $V_c(AE \approx 100$ nT) $\approx$ 50 km/s). Therefore this BBF event is composed of three FBs. The FBs are centered at around 2346:30, 2349:30, and 2352:30 UT. The first one has a rise time of about a minute but is not as sharply defined as the other two. The second and third one have a FWHM duration of about 1 min.

Lack of a theoretical model of generation and evolution of the FBs and the BBF events makes it difficult to justify the practical definition of the FBs and the BBFs used in this paper. For example, it is not clear whether the 10-30 s time scale local

velocity maxima around 2351 UT should be considered as multiple FBs separated by periods shorter than their duration or merely higher-order perturbations of the plasma flow velocity within a single FB. Trying to be operational (yet leave room for constructive future reconsideration of the phenomenology), we will not concern ourselves with time scales less than of the order of a minute (thus viewing the structure as a single FB), but we will continue to use the 5-s resolution data in all our analyses of the FB and BBF structures.

Case studies like the present one also reveal that flows below the 400-km/s level are an integral part of the BBF structure. The 400-km/s threshold does not represent a physically significant quantity. It is kept in this paper for reasons of convenience in selecting case studies for visual inspection from the entire data base and, in addition, to aid the comparison between our results and the statistical findings of BJetal90.

The magnetic field magnitude dropped below the 5-nT level several times during this interval. During one of these times (at around 2346:45 UT, indicated by the arrow on top of the velocity trace) the 3D ion distribution function was transmitted to the ground and was included in the work by *Nakamura et al.* [1991] as an example of a neutral sheet ion distribution that demonstrates an atypical, beamlike behavior (their Figure 12). A beamlike behavior, which was seen only twice in their entire data set, signifies a distribution function whose peak is at a velocity larger than the thermal velocity of the distribution (see their Figure 12 and the associated discussion). It is noteworthy that this distribution was sampled closest to the peak of the first identifiable FB during this BBF. (We would like to remind the reader that the above authors used unaveraged 4.5-s resolution data whereas the data set that we used for visual inspection was composed of 5-s averages of the original data set.) It is also important to mention that the velocity at the peak of the distribution was 1700 km/s, which exceeds the thermal speed of 1400 km/s, but the fastest bulk flow during a 5-min time period around the event was 629 km/s (see their Table 1, event 27). Therefore the ion distribution may exhibit a beamlike behavior but it still corresponds to a subsonic flow.

The magnetic field was highly variable down to the 5-s time scale, especially near the neutral sheet (i.e., when its magnitude was small). Occasionally, B_z turned southward, but for very short intervals as evidenced by the transient changes in the sign of θ_B. At other times, B_x changed sign (i.e., when $0° < \phi_B < 90°$ or $270° < \phi_B < 360°$ from its original taillike ($\phi_B \approx 180°$) orientation); a signature that suggests neutral sheet crossings. However, the most prominent feature of the magnetic field during the BBF event is the presence of large, transient dipolarizations that are most markedly evidenced by the increases in the elevation angle θ_B. Such features have been noted in all but four of the BBF events that we inspected visually. If we interpret the magnetic field variability as temporal, we can estimate the time rate of change of the magnetic field $\delta B/\delta t$ during these dipolarizations. For example, the dipolarization that occurred at 2343:30 and was associated with a magnetic field almost completely in the z direction, would yield an estimate for $\delta B/\delta t$ during the particular BBF event that we selected to present of $\approx$ 15 nT/30 s $\approx$ 0.5 nT/s.

The large variability in both the magnitude and direction of the magnetic field has the following implications: First, distinguishing between temporal (i.e., $\delta B/\delta t \neq 0$) and spatial evolution becomes problematical. Second, quantities like the angle between the plasma velocity and magnetic field or the ion beta that are derived from and depend sensitively on the magnetic field orientation or magnitude are going to reflect this variability.

The ion density exhibited fluctuations on a time scale of a few minutes that seem uncorrelated with the velocity peaks. The ion temperature increased by a factor of 2.5 from the beginning of the BBF event to the first velocity peak and remained fairly constant afterward (except for a minute-long interval around 2350:00 UT). During the same time the electron temperature increased also but the ratio of the ion to electron temperature (T_i/T_e) remained constant within 25% of its average value (8.8) over the entire interval. This is in agreement with the results of BJetal89 and *Christon et al.* [1991], who found that a good statistical correlation between the ion and the electron temperatures exists in the near-Earth plasma sheet. Finally, the total (ion+electron+magnetic) pressure also remained fairly constant down to time scales of tens of seconds; variations at a shorter time scale do not show any correlation with the flow bursts.

Let us now describe several features of the BBF event that emerge from an analysis of the time evolution of the plasma and magnetic field during this plasma sheet crossing. At 2342:00 UT the spacecraft was located south of the neutral sheet and was moving toward it, while the ion velocity was starting to increase. Nonspatial changes in B were already apparent at around 2343:30 UT, when the field temporarily increased in magnitude and at the same time dipolarized. This transient dipolarization ended within a minute. (Unlike what happened in the rest of the interval, this dipolarization coincided with a decrease in the velocity magnitude.) The spacecraft approached the neutral sheet at around 2345:30 UT and remained near it until about 2350:00 UT. During that time it sampled the three FBs and detected associated B_z fluctuations (many of which correspond to dipolarizations).

At 2350:00 UT the flow velocity dropped sharply to <100 km/s, and the magnetic field assumed values comparable to the ones that it had prior to the BBF onset both in magnitude and in direction. An associated decrease in the ion temperature supports the interpretation that the spacecraft temporarily exited to the outermost central plasma sheet. It is then reasonable to conclude that the decrease in the velocity may have occurred, at least partly, as a result of a spatial effect: motion of the spacecraft away from a region of enhanced flow confined close to the neutral sheet. (A temporal change of the velocity that had already started before 2350:00 UT could have been continuing and could also be partly responsible for the sharp velocity change that we saw.) Reentry to the neutral sheet marked the onset of yet another increase in the velocity magnitude and a magnetic field that was almost completely in the z direction.

At around 2353:00 UT the velocity magnitude decreased abruptly after reaching a peak of $\approx$ 900 km/s. The flow velocity remained almost completely in the x direction (as evidenced by the sudden change of the value of ϕ_V from 0° to 180°: V_x changed from $\approx$ 900 to $\approx$ –200 km/s within $\approx$ 50 s). The ion density, ion temperature, and magnitude of the magnetic field were variable but uncorrelated with the dramatic decrease of the velocity. We interpret this sharp, unidirectional velocity change as genuinely temporal, since there is no evidence that the spacecraft suddenly crossed from one plasma sheet region to another during this time. In particular, the magnetic field orientation remained dipolelike during this dramatic velocity change.

One may note that the spectacular FB of 2352:30 UT is not, strictly speaking, associated with dipolarization, but with an already (almost) completely dipolarized magnetic field. The increase in the elevation angle ϕ_B took place for the most part concurrently with the reentry of the satellite from the outermost central plasma sheet to the vicinity of the neutral sheet, about 90 s prior to the FB peak. Time lags between the dipolarization signature and the FB peak occurrence are often encountered in our data set. At other (less frequent and hence exceptional) occasions, FBs are not accompanied by a magnetic field dipolarization at all. It is not obvious whether the 2352:30 UT flow burst is an example of a FB exhibiting a large time lag from its associated dipolarization or an exceptional event.

A few minutes after the tailward shift of the velocity the magnetic field increased and assumed its original, taillike orientation and the flows became smaller, less bursty and of more variable direction.

2.2.3. *CPS regions.* Figure 3 includes a breakdown of the CPS crossing into ICPS and OCPS based on the BJetal90 selection criteria. Overall, there is agreement between the classification of the samples into the two CPS regions and the impression gained from the detailed analysis of the plasma and magnetic field quantities: Prior to and after the BBF event the spacecraft was located in the OCPS; throughout the BBF event the spacecraft was predominantly in the ICPS apart from a short-lived exit to the OCPS at 2350 UT. However, two other transient exits to the OCPS (at 2344:30 UT and at 2359:30 UT) may simply reflect the enhanced temporal variability of the magnetic field.

The distinction between ICPS and OCPS is justified in a statistical study as an indicator of the distance from the neutral sheet. However, for the purposes of the case studies that we undertake a breakdown of the BBF structure (and FB occurrence) into ICPS- and OCPS-related portions may be unphysical and misleading: unphysical, because the boundary between the ICPS and OCPS is not a topological boundary (in contrast to the CPS-PSBL boundary which signifies the transition between reconnected and currently reconnecting field lines); misleading, because the BBF-associated magnetic field variability and the FB-associated dipolarizations may reflect on the (strictly) magnetic field criterion that separates the CPS regions. Therefore within individual BBF events we will not make an attempt to distinguish between the different CPS regions as put forth in the statistical studies of BJetal89 and BJetal90. However, we would like to remind the reader that we have used the "ICPS criterion" to select the events that we analyzed in an effort to include high-speed flows that are, at least partially, close to the neutral sheet.

2.2.4. *BBF contribution to transport.* In order to assess the contribution of the BBFs to plasma sheet transport within the magnetotail and to interpret their significance for magnetosphere-ionosphere coupling, we plot a set of derived magnetohydrodynamic quantities in Figure 4. These are calculated from the instantaneous (5-s resolution) values of the measured plasma moments and magnetic field described in Figure 3. The formulae used for the calculations appear in the figure caption. The calculations of the electric field $\mathbf{E}$ and the energy flux density $\mathbf{Q}$ are based on the MHD approximation $\mathbf{E} = -\mathbf{V}\times\mathbf{B}$, and therefore these quantities are meaningful only at time scales larger than the local ion gyroperiod.

Figures 4*a* and 4*c*, which show the sonic and Alfvén Mach numbers of the flow, indicate that the flow was everywhere subsonic but close to the local Alfvén speed during most

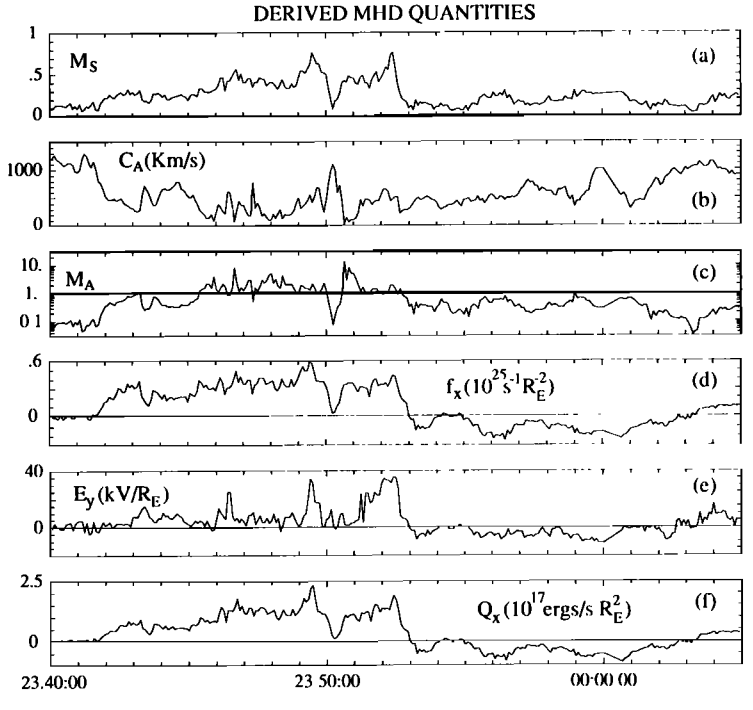

Fig. 4. Quantities derived from the measured magnetic field and plasma data of Figure 3. Shown from top to bottom are: the sonic Mach number defined as $M_s = V_i\left(\frac{5}{3}kT_i/m_i\right)^{-1/2}$, where m_i is the proton mass; the Alfvén speed $C_A = B_t(4\pi N_i m_i)^{-1/2}$; the Alfvén Mach number $M_A = V_i/C_A$ and the reference line $M_A = 1$; the x component of the particle flux $\mathbf{f} = N_i\mathbf{V}$ and the reference line $f_x = 0$; the y component of the electric field $\mathbf{E} = -\mathbf{V}\times\mathbf{B}$ and the reference line $E_y = 0$; the x component of the energy flux density $\mathbf{Q} = \frac{1}{2}\rho V^2\cdot\mathbf{V} + \frac{5}{2}(P_i + P_e)\cdot\mathbf{V} + \frac{c}{4\pi}(\mathbf{E}\times\mathbf{B})$ and the reference line $Q_x = 0$.

of the high-speed interval. The sharp peaks in the Alfvén Mach number correspond to places where the Alfvén velocity (Figure 4*b*) became extremely small.

The x component of the particle flux $\mathbf{f}= N_i\mathbf{V}$ is shown in Figure 4*d*. Averaging f_x over the 25 minute interval shown, gives a value for the earthward particle flux of $\overline{f_x} \approx 10^{24}\mathrm{s}^{-1}R_E^{-2}$. This average includes contributions from the large earthward flux prior to 2353:00 and the smaller tailward flux after the reversal of the velocity. The average flux should be compared to the total earthward particle transport across the entire plasma sheet for similar geomagnetic conditions (based on the level of *AE*), which is of the order of $7 \times 10^{25}\mathrm{s}^{-1}$ given an average density of $0.3\ \mathrm{cm}^{-3}$, an average velocity of 50 km/s and a cross-sectional area of $30 \times 4\ R_E^2$, at a downtail distance of $\geq 14\ R_E$ (see Figure 4 of BJetal89; also Figure 3 of *Huang and Frank* [1986] for comparison). For a $10\ R_E^2$ scale size in the y-z GSM plane the particle average flux over the 25-min interval of the BBF event is a sizeable fraction of the total particle flux across the magnetotail. This suggests that BBFs are localized.

The y component of the $-\mathbf{V}\times\mathbf{B}$ electric field (which is the dominant component of $\mathbf{E}$ during this and most of the BBF events that we have inspected) is shown in Figure 4*e*. An estimate of the expected cross-tail electric field based on the empirical formula of *Kivelson* [1976], gives $E = 0.46/(1 - 0.082K_p)^2\,\mathrm{kV}/R_E \approx 1\mathrm{kV}/R_E$, for the values of K_p quoted during this plasma sheet crossing. It can be seen that the derived electric field during the BBF event is intermittently very large compared to the expected dawn-dusk electric field value. If such a large electric field were to extend across the whole tail it would give unrealistically large values for the cross-tail potential. This also suggests that the BBF events may be localized in the y direction.

The large electric fields derived are not inconsistent with an inductive origin, given the observed level of magnetic field variations ($0.5\,\mathrm{nT/s} \sim 20\,\mathrm{kV}/R_E^2$). They also represent a large magnetic flux transport per unit y distance ($\partial\Phi/(\partial t\Delta y) \sim 2. \times 10^4\ \mathrm{Wb}/(\mathrm{s}\cdot R_E)$) in the earthward direction. For a $3\ R_E$ scale size in the y direction, the flux transport rate would be a significant fraction of the rate of the polar cap flux increase during the growth phase of a substorm which is of the order of $\partial\Phi/\partial t \sim 2. \times 10^5$ Wb/s [e.g., *Holzer and McPherron*, 1986].

Figure 4*f* shows the x component of the energy flux density $Q_x = \frac{1}{2}\rho V^2 \cdot V_x + \frac{5}{2}(P_i + P_e)\cdot V_x + \frac{c}{4\pi}(\mathbf{E}\times\mathbf{B})_x$ associated with the BBF event. The dominant term in this quantity is the thermal energy transport term, which is proportional to $(P_i + P_e)V_x$. Integrating under the curve to estimate the net energy associated with the event, we get an earthward energy per unit BBF area in the y-z plane of $\sim 4. \times 10^{19}\mathrm{ergs}/R_E^2$. This number suggests that either the BBF activity is highly localized (area $\lesssim 10R_E^2$), or the total earthward energy transport associated with it is comparable with the $\sim 2.8 \times 10^{21}$ergs total energy released due to auroral precipitation and Joule heating dissipation during substorms [*Akasofu*, 1977].

2.3. *Other BBF Events*

We now turn to the question of whether the properties of the low-*AE* BBF events extend to the high-*AE* BBF events. This question is particularly important since the data base on which we rely for analysis of individual events (this section), as well as the entire 2-year data base which is used for the superposed epoch analysis (next section), is dominated by BBFs that occur during "active" times. We concentrate on the systematic features of the profiles of the magnetic field and the ion velocity during the BBF events because they reveal properties which are not evident in a statistical study.

Figure 5 shows 5-s averages of the magnetic field and ion velocity during four BBF events (events B-E of Figure 1). Two of them occur during the expansion phase of moderate substorms (events B and D) and two of them occur during low-*AE* intervals (events C and E). Notice that the panels are plotted on different scales for different events. Gaps in the data have been removed by linear interpolation. The grey-scale bar above each magnetic field panel indicates the magnetotail region that the spacecraft was traversing, based on the BJetal90 selection criteria. The criteria have been applied to the degapped data. The three arrows above the velocity traces of events B and E correspond to times when the ion distribution functions were transmitted and included in the work of *Nakamura et al.* [1991] (see their Figures 5, 19, and 11 respectively).

It is evident from this figure that the transient dipolarizations, the large magnetic field variability and the bursty, large, earthward flows are properties characteristic of the BBF events irrespective of the concurrent value of *AE*. The abrupt velocity enhancements have similar time scales in all cases (order of 1 min) and can therefore be identified with flow bursts. Most FBs are clearly defined from their FWHM duration (this is the case in event D). Others are not so easily identifiable possibly because their separation in time may be comparable to or less than their duration (as could be the case with event B at around 0208:30 UT). If the spacecraft is in the plasma sheet prior to the onset of the flow enhancement and remains within it after the flow subsidence (events B and C), the enhanced flow time scale (BBF time scale) is of the order of 10 min. However, the BBF time scale is difficult to assess if motions of the plasma sheet do not allow the detection of the entire event (as may be the case in events D and E).

It is important to mention the peculiarities of certain BBF events of Figure 6 that pertain to the BJetal90 selection criteria used in our paper.

Event B corresponds to an expansion phase of a substorm, during which the partial densities of the 1.8–30 keV electrons and 8.5–40 keV ions (not shown) are above the two-count level, therefore the data segment belongs to the plasma sheet. A reduction of the magnetic field magnitude prior to the BBF onset and transient dipolarizations associated with the event result in a field that is completely in the z_{GSM} direction during most of the 25-min interval. As a result, the "ICPS criterion" ($B_{xy} < 15$nT or $B_z/B_{xy} > 0.5$ for the sample to belong in the ICPS) is satisfied. The plasma density (not shown), however, is low and results in existence of photoelectrons and occasional imbalance between the ion and electron densities. As a result the "photoelectron criterion" ($N_e > N_i^{0.86}$ for the sample to belong to the PSBL) is also satisfied several times throughout the event. The criteria applied in this paper (in accordance with the BJetal90 analysis) classify this interval as a low-density ICPS rather than a completely dipolar PSBL interval. This is, apparently, not the conclusion of *Nakamura et al.* [1991], where the distribution function sampled at 0205:30–0206:00 UT (see their Figure 19) is considered as an example of a typical, bean-shaped, PSBL distribution function.

That the distribution functions at the neutral sheet can, at times, exhibit a beamlike behavior reminiscent of unidirectional streaming PSBL distributions has been pointed out by both *Huang and Frank* [1987] and *Nakamura et al.*

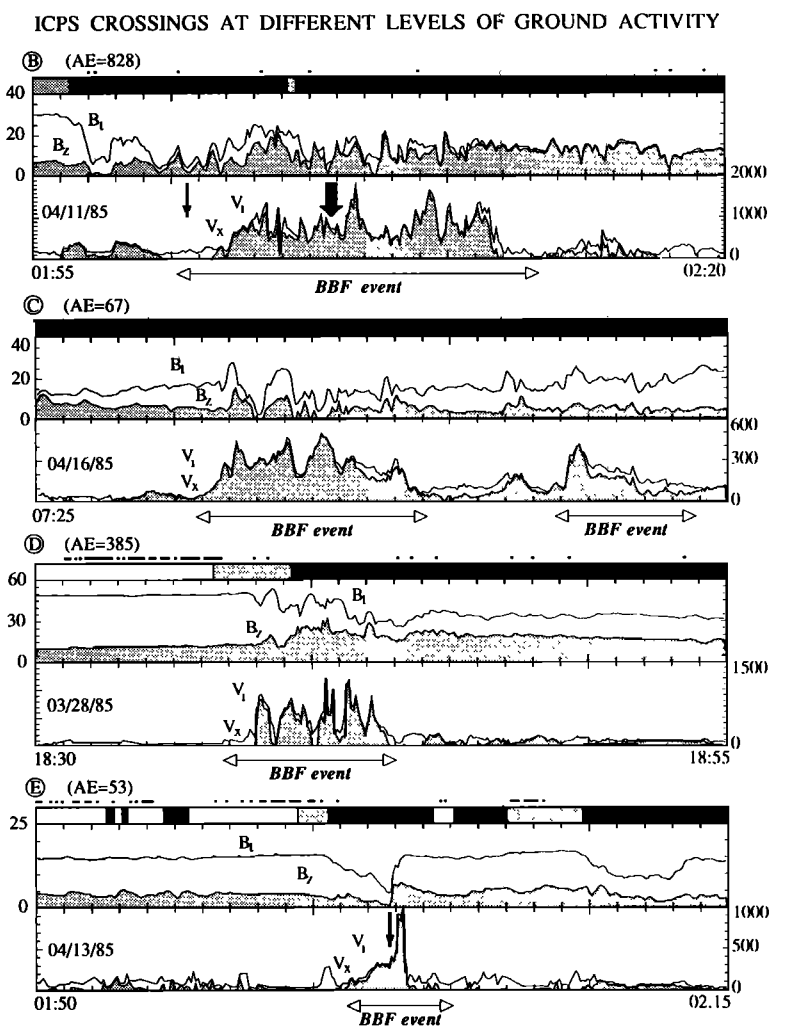

Fig. 5. BBF events detected on AMPTE/IRM for times of different *AE* levels. Events are labeled B,C,D,E and correspond to the labeled arrows of Figure 1; 5-s resolution data are plotted for a 25-min interval during each crossing. For each encounter shown are: a grey-scale bar that indicates the tail region where the spacecraft was located (same as in Figure 2.); the magnetic field magnitude B_t (nanoteslas, top trace) and the GSM z omponent B_z (nanoteslas, bottom and filled trace); the velocity magnitude V_i (kilometers pes second, top trace) and x component V_x (kilometers pes second, bottom and filled trace). Data gaps have been removed using linear interpolation. Times during which the BJetal90 selection criteria could not characterize, prior to degapping, the samples unambiguously (because of data gaps) have been marked with dots that appear above each grey-scale bar.

[1991]. However, the convective nature of the flows at the ICPS (see BJetal90, Figure 9) renders them far more effective for flux transport and reduction of the available cross-tail potential.

Event E corresponds to a quiet day plasma sheet encounter, during which a transitory reduction of the magnetic field magnitude to a value of 4 nT, interpreted as an ephemeral approach to the neutral sheet, is accompanied by a strong earthward flow. During much of the 25-min interval shown the "ICPS criterion" is satisfied. However, the partial electron (1.8-30 keV) and ion (8.5-40 keV) densities (not shown) occasionally decrease below the two-count level. This results in a classification of certain samples as lobe cases (e.g., between 0204:20 and 0205:10 UT) and in ostensible lobe-CPS transitions (also at 0152:30 UT and at 0154:35 UT). These transitions are not accompanied by significant changes of the magnetic field magnitude or topology (which provide an indication of the distance to the neutral sheet). Hence they can be interpreted as dynamical changes of the plasma that populates flux tubes at a constant distance from the neutral sheet.

SUPERPOSED EPOCH ANALYSIS

In this section we will show that several of the characteristics of the plasma sheet during BBF events derived from visual inspection of the 1985 case studies and described for one case in the previous section, also appear consistently in a statistical manner in the AMPTE/IRM plasma sheet crossings from the years 1985–1986.

Our statistical treatment of the entire 1985–1986 data base of AMPTE/IRM plasma sheet crossings applies the superposed epoch analysis technique to the data at 4.5-s resolution. In this analysis, each local peak in the velocity magnitude that was above 400 km/s and occurred in the ICPS (as defined in BJetal90) and within $|Y_{GSM}| < 15\ R_E$ and $X_{GSM} < -9\ R_E$ constituted a single event. (For example, in the BBF event of Figure 3 there are 3 FBs but 16 local velocity peaks. Each of these velocity local maxima were considered to be

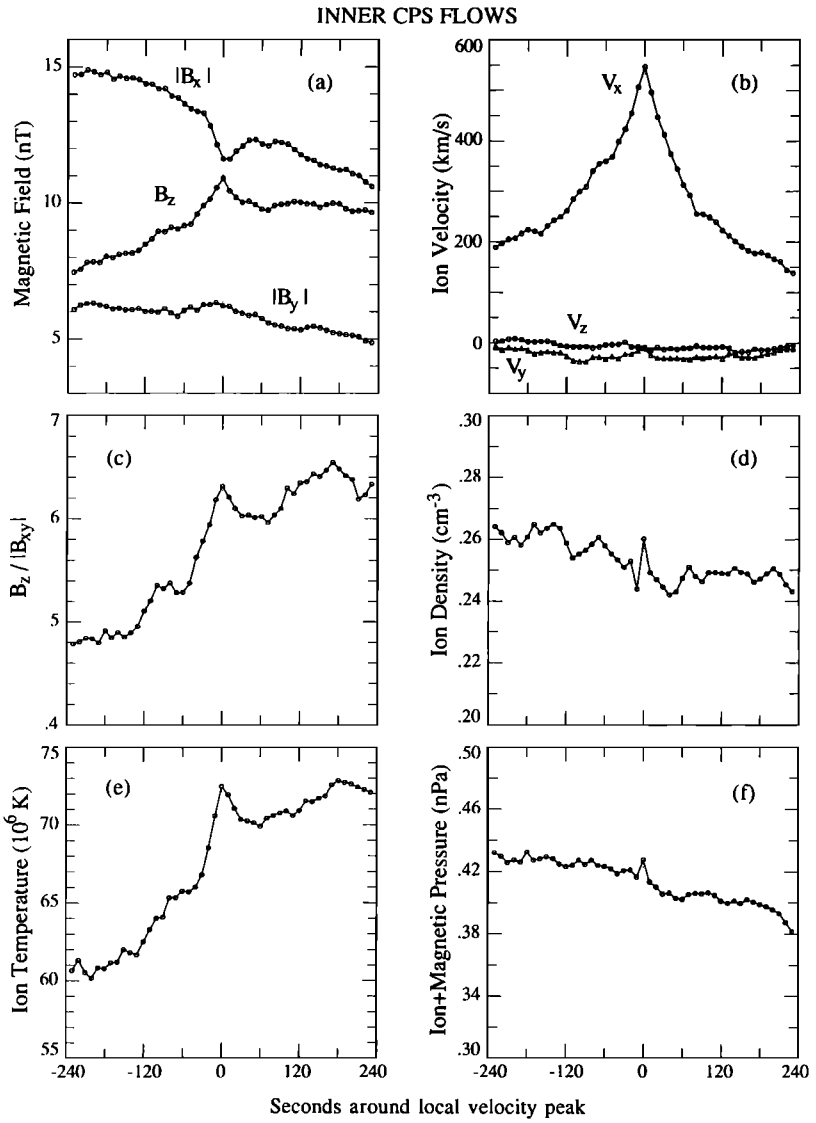

Fig. 6. Results of the superposed epoch analysis applied on plasma and magnetic field data around ICPS local velocity peaks above 400 km/s of the 1985–1986 AMPTE/IRM data base. The plasma and magnetic field data were time centered around each velocity peak (t=0) and averaged over the data base from –4 to +4 min. Shown are the resulting traces at 10-s resolution.

independent events in this analysis.) The events were time centered around their velocity peaks. Data for all events were ordered relative to their center time (t = 0) and the average values of the quantities of interest (e.g., B_z) were calculated for every 4.5-s starting from 4 min before and ending 4 min after the time t = 0. The resulting 4.5-s resolution traces were block averaged at 10-s resolution.

Figure 6 shows the results of the superposed epoch analysis applied to the components of the magnetic field, the ion velocity, density, and temperature, and the sum of the ion and magnetic field pressure (which is very close to the total pressure). In order to remove dawn-dusk (north-south) asymmetries in the magnetic field the method was applied to the absolute value of B_y (B_x).

The average velocity profile around the velocity peaks is presented in Figure 6*b*. It is evident from the time scale of the rise and fall of the velocity that the FBs (time scale of the order of 1 min) dominate the profile of the velocity. More than one local velocity maxima can occur within the ±4-min interval around each event, as well as more than one FBs (for example within ±4 min around the peak of the FB occurring at 2352:30 there are seven velocity peaks one of which is the peak of a FB). However, it appears that the local velocity peaks are in general statistically uncorrelated. As a result, although the sharp peak within about ±1 min around t = 0 confirms statistically our previous association of the flow bursts with the order of a minute time scale, the spread introduced due to the overlap of the events makes the FWHM of the FB larger than 1 min (FWHM is $\approx$ 3 min).

The flow at the peak is almost completely in the X_{GSM} direction. The V_y component of the velocity is small and becomes even smaller at the peak of the FB. The V_z component is almost zero. As a result the superposed velocity vector at t = 0 is within 6° of the sunward direction. The BBF event, however, defined as the interval during which the flow speeds exceed the long-term average of 50 km/s, lasts for quite a few minutes. The flow in Figure 6*b* does not subside to average convection values even 4 min after the occurrence of the velocity peak. We find no significant difference in the velocity profiles when we repeat the analysis for the lower velocity (400 km/s < V_i < 500 km/s) and the higher velocity (500 km/s < V_i < 1000 km/s) subsets of the data base.

The magnetic field profile presented in Figure 6*a* shows that, on the average, a clear decrease in $|B_x|$ and a clear increase in B_z correlate with the FBs. This signature of more pronounced dipolarization on the FB time scale seems to be embedded in a BBF time scale dipolarization that remains after the occurrence of the FB. This remnant dipolarization can be noted during many BBF events (roughly 50% of the 1985 case studies) by visual inspection. However, during the rest of the cases the elevation angle resumes its pre-BBF value suggesting that the dipolarizations are only transient (e.g., the event analyzed in detail in this paper). The BBF time scale dipolarization suggests that the BBF activity may, at times, be associated with irreversible changes of the plasma sheet configuration.

An additional diagnostic that illustrates the dipolarization signature during BBF events is the ratio $B_z/|B_{xy}|$ plotted in Figure 6*c*. This diagnostic also indicates that the correlation between FBs and dipolarization of the magnetic field is not a result of a statistical bias toward events with large magnetic field magnitude.

Figures 6*d* and 6*f* show that the FB activity can be described to zeroth order as incompressible. The temperature, shown in Figure 6*e*, exhibits a peak correlating with the FB peak, superposed on a general increasing trend. This behavior, which is consistent with the general behavior of BBFs drawn from case studies, is the second of the plasma sheet characteristics associated with BBFs consistent with irreversibility.

In order to evaluate the (somewhat subjective) conjecture that the BBF events A-E of Figure 1 are representative of the entire data base, we applied the superposed epoch analysis technique on the data set that contained only these BBF events. Despite the limited number of local velocity maxima (and FBs) contained in this data set, the trends of the ion velocity, the magnetic field dipolarization (B_z/B_{xy}), the ion temperature, and the total pressure are qualitatively similar to the ones shown in Figure 6. (The ion density exhibits an anticorrelation with the velocity peak.)

By applying the superposed epoch analysis technique to subsets of the entire data base we can extract information about the spatial dependence of the events that show the behavior described above. This procedure reveals that the subsets of the center tail ICPS high-speed flows ($X_{GSM} < -14\ R_E$, $|Y_{GSM}| < 5\ R_E$), the distant-tail, CPS high-speed flows ($X_{GSM} < -14\ R_E$), and the distant-tail, CPS high-speed flows mostly perpendicular to the magnetic field (angle of velocity to magnetic field >45° during peak of velocity) exhibit characteristics in their superposed quantities similar to those of Figure 6. Superposed epoch analysis applied on mostly parallel, distant-tail, CPS local velocity maxima does not reveal a discernible dipolarization signature. The data base is dominated by dusk events, as a result of the orbital bias of the satellite; separating the fewer dawn samples and applying the analysis on that data set results in traces with very large variability that prevents us from extracting a clear pattern.

SUMMARY AND CONCLUSIONS

The statistical analyses of BJetal89 and BJetal90 have shown that there exists a class of plasma sheet flows that has distinctly different characteristics from the PSBL flows. These high-speed flows occur in the ICPS, are thought of as bulk flows of the plasma sheet population, they are predominantly earthward (when large), mostly perpendicular to the instantaneous magnetic field and occur even for low-*AE* values. In this paper we used AMPTE/IRM data from a representative case and superposed epoch analysis on data from a 2-year data base to describe the evolution of the magnetic field and plasma during such events.

We have shown that the high-speed flows occur as part of 10-min time scale enhanced flow intervals, during which the velocity exhibits large amplitude peaks of order of a minute time scale. We termed the enhanced flow intervals bursty bulk flow events and the velocity peaks flow bursts. We have argued that both temporal and spatial effects are responsible for the intermittent nature of the flow bursts. The FBs are typically associated with increased magnetic field variability, with transient dipolarizations, and with ion heating.

One would be tempted to interpret the FBs as evidence of nearby, localized (in the *x*-*y* plane), bursty reconnection. We abstain from such an interpretation for two reasons. First, it is evident from Figures 2 and 3 that the FBs can take place within a plasma sheet that is never severed. Whenever its outer portion (OCPS) is sampled (for example, at 2350 and at 0003 UT), it has the same field topology. Although we are not able to distinguish between constrictions/dilations of the plasma sheet and tail oscillations, the fact remains that the plasma sheet retains its integrity during the BBF event. The sharp flow reversal of 2353:00 might suggest that an X line moved (earthward) past the spacecraft if the reconnection interpretation were to be applied. However, B_z remained large and positive immediately after the flow reversal and never changed sign in the subsequent interval.

Although our data base contains a multiplicity of BBFs, each associated with different *AE* levels, different substorm phases, and presumably solar wind conditions, we believe that the event presented in this paper has features common to all. That this BBF event occurred during a low-*AE* interval and the fact that the spacecraft was inside the plasma sheet before, during and after the event, suggest that BBFs may be important to plasma sheet transport not only during large-scale substorms but also in general.

In conclusion, we note that *Erickson and Wolf* [1980] suggested that steady convection may not be possible within the plasma sheet. These authors argued that, if plasma sheet flux tubes moving earthward in a taillike magnetic field are compressed adiabatically, they would fail to remain in pressure equilibrium with the lobes. Theoretical attempts to resolve this problem [e.g. *Kivelson and Spence*, 1988; *Pritchett and Coroniti*, 1990; *Pontius and Wolf*; 1990] have not yet led to a conclusive answer. The above definition of a "pressure crisis" as well as the theoretical efforts to address it for quiet times have been based on the assumption that convection, if it exists, would be steady and therefore consistent with a steady (in space and time) cross-tail electric field. However, BJetal89 argued that the low average velocity (and therefore the "steady convection") in the plasma sheet is, in reality, a superposition of bursty, high-speed flows with "intermittent intervals of nearly stagnant plasma." Our analysis takes the statistical results of BJetal89 further and suggests that if BBF events have a cross section of the order of a few tens of R_E^2 they can accomplish earthward mass, energy, and flux transport comparable with that expected from "steady state convection" across the entire plasma sheet. It should be noted, though, that BBFs of size smaller than 10 R_E^2 with the appropriate occurrence frequency could accomplish the same transport. (Our one-satellite observations cannot distinguish between the two pictures.) It seems, then, worthwhile to investigate whether convection in the plasma sheet proceeds

in an unsteady manner, principally by means of short bursts (FBs) of 1-min time scale that occur during 10-min time scale periods of spatially localized ($\lesssim 10\ R_E^2$) convection enhancements (BBFs).

Acknowledgments. We would like to gratefully acknowledge valuable discussions with S. H. Chen, K. Khurana, J. Gosling, R. L. McPherron, A. Roux, R. Sagdeev, and V. Troitskaya. The help of Hsien-Shien Chen with the AMPTE/IRM data processing was greatly appreciated. We would also like to acknowledge the NSSDC for providing the 5-s averages of the AMPTE/IRM data and the NOAA for providing the *AE* index time-series. The work of C.F.K., F.V.C., R.P., and V.A. was supported by NASA through grant NAGW 1624. M.G.K. was supported by NSF through grant ATM 89-13342. R.J.W. was supported by the NASA grant NAG 5-1530.

The editor thanks S. P. Christon and J. A. Slavin for their assistance in evaluating this paper.

REFERENCES

Akasofu, S.-I., *Physics of Magnetospheric Substorms*, p. 274, D. Reidel, Hingham, Mass., 1977.

Baumjohann, W., G. Paschmann, N. Sckopke, C. A. Cattell, and C. W. Carlson, Average ion moments in the plasma sheet boundary layer,*J. Geophys. Res., 93,* 11,507–11,520, 1988.

Baumjohann, W., G. Paschmann, and C. A. Cattell, Average plasma properties in the central plasma sheet, *J. Geophys. Res., 94,* 6597–6606, 1989.

Baumjohann, W., G. Paschmann, and H. Lühr, Characteristics of high-speed ion flows in the plasma sheet, *J. Geophys. Res., 95,* 3801–3809, 1990.

Caan, M. N., D. H. Fairfield, and E. W. Hones, Magnetic fields in flowing magnetotail plasmas and their significance for magnetic reconnection, *J. Geophys. Res., 84,* 1971–1976, 1979.

Christon, S. P., D. J. Williams, D. G. Mitchell, C. Y. Huang, and L. A. Frank, Spectral characteristics of plasma sheet ion and electron populations during disturbed geomagnetic conditions, *J. Geophys. Res., 96,* 1–22, 1991.

Coffey, H. E., Geomagnetic and solar data, *J. Geophys. Res., 90,* 7635, 1985.

Coroniti, F. V., L. A. Frank, R. P. Lepping, F. L. Scarf, and K. L. Ackerson, Plasma flow pulsations in the earth's magnetic tail, *J. Geophys. Res., 83,* 2162–2168, 1978.

Coroniti, F. V., L. A. Frank, D. J. Williams, R. P. Lepping, F. L. Scarf, S. M. Krimigis, and G. Gloeckler, Variability of plasma sheet dynamics, *J. Geophys. Res., 85,* 2957–2977, 1980.

DeCoster, R. J., and L. A. Frank, Observations pertaining to the dynamics of the plasma sheet, *J. Geophys. Res., 84,* 5099–5121, 1979.

Eastman, T. E., L. A. Frank, W. K. Pederson, and W. Lennartsson, The plasma sheet boundary layer, *J. Geophys. Res., 89,* 1553–1572, 1984.

Eastman, T. E., L. A. Frank, and C. Y. Huang, The boundary layers as the primary transport regions of the Earth's magnetotail, *J. Geophys. Res., 90,* 9541–9560, 1985.

Erickson, G. M., and R. A. Wolf, Is steady state convection possible in the earth's magnetotail ?, *Geophys. Res. Lett., 7,* 897–900, 1980.

Forbes, T. G., E. W. Hones, Jr., S. J. Bame, J. R. Asbridge, G. Paschmann, N. Sckopke, and C. T. Russell, Evidence for the tailward retreat of a magnetic neutral line in the magnetotail during substorm recovery, *Geophys. Res. Lett., 8,* 261–264, 1981.

Hayakawa, H., A. Nishida, E. W. Hones, Jr., and S. J. Bame, Statistical characteristics of plasma flow in the magnetotail, *J. Geophys. Res., 87,* 277–283, 1982.

Holzer, R. E., and R. L. McPherron, A quantitative empirical model of the magnetospheric flux transfer process, *J. Geophys. Res., 91,* 3287–3293, 1986.

Huang, C. Y., and L. A. Frank, A statistical study of the central plasma sheet: Implications for substorm models, *Geophys. Res. Lett., 13,* 652–655, 1986.

Huang, C. Y., and L. A. Frank, Reply to Cattell and Elphic, *Geophys. Res. Lett., 14,* 776–778, 1987.

Huang, C. Y., L. A. Frank, and T. E. Eastman, Plasma flows near the neutral sheet of the magnetotail, in *Magnetotail Physics*, edited by A. T. Lui, pp. 127–135, Johns Hopkins University Press, Baltimore, Md., 1987.

Kivelson, M. G., Magnetospheric electric fields and their variation with geomagnetic activity, *Rev. Geophys. Space Phys., 14,* 189–197, 1976.

Kivelson, M. G., and H. E. Spence, On the possibility of quasi-static convection in the quiet magnetotail, *Geophys. Res. Lett., 15,* 1541–1544, 1988.

Lühr, H., N. Klöcker, W. Oelschlägel, B. H., B. Häusler, and M. Acuña, The IRM fluxgate magnetometer, *IEEE Trans. Geosci. Remote Sens., GE-23,* 259–261, 1985.

Lui, A. T. Y., T. E. Eastman, D. J. Williams, and L. A. Frank, Observations of ion streaming during substorms, *J. Geophys. Res., 88,* 7753–7756, 1983.

Nakamura, M., G. Paschmann, W. Baumjohann, and N. Sckopke, Ion distributions and flows near the neutral sheet, *J. Geophys. Res., 96,* 5631–5649, 1991.

Paschmann, G., H. Loidl, P. Obermayer, M. Ertl, R. Laborenz, N. Sckopke, W. Baumjohann, C. W. Carlson, and D. W. Curtis, The plasma instrument for AMPTE/IRM, *IEEE Trans. Geosci. Remote Sens., GE-23,* 262–266, 1985.

Pedersen, A., C. A. Cattell, C.-G. Fälthammar, K. Knott, A. A. Lindqvist, R. H. Manka, and F. S. Mozer, Electric fields in the plasma sheet and plasma sheet boundary layer, *J. Geophys. Res., 90,* 1231–1242, 1985.

Pontius, D. H., Jr., and R. A. Wolf, Transient flux tubes in the terrestrial magnetosphere, *Geophys. Res. Lett., 17,* 49–52, 1990.

Pritchett, P. L., and F. V. Coroniti, Plasma sheet convection and the stability of the magnetotail, *Geophys. Res. Lett., 17,* 2233–2236, 1990.

Pytte, T., R. L. McPherron, E. W. Hones, Jr., and H. I. West, Jr., Multiple satellite studies of magnetospheric substorms: Distinction between polar magnetic substorms and convection-driven negative bays, *J. Geophys. Res., 83,* 663–679, 1978.

Russell, C. T., and K. I. Brody, Some remarks on the position and shape of the neutral sheet, *J. Geophys. Res., 72,* 6104–6106, 1967.

Sergeev, V. A., O. A. Aulamo, R. L. Pellinen, M. K. Vallinkoski, T. Bösinger, C. A. Cattell, R. C. Elphic, and D. J. Williams, Non-substorm short-lived injection events in the ionosphere and magnetosphere, *Planet. Space Sci., 38,* 231–239, 1990.

Slavin, J. A., E. J. Smith, D. G. Sibeck, D. N. Baker R. D. Zwickl, and S.-I. Akasofu, An ISEE 3 study of average and substorm conditions in the distant magnetotail, *J. Geophys. Res., 90,* 10,875–10,895, 1985.

Slavin, J. A., P. W. Daly, E. J. Smith, T. R. Sanderson, K. -P. Wenzel, R. P. Lepping, and H. W. Kroehl, Magnetic configuration of the distant plasma sheet: ISEE 3 observations, in *Magnetotail Physics*, edited by T. A. Lui, pp. 59–63, Johns Hopkins Univ. Press, Baltimore, Md., 1987.

V. Angelopoulos, F. V. Coroniti, C. F. Kennel, and R. Pellat, Department of Physics, University of California, Los Angeles, CA 90024–1567.

W. Baumjohann and G. Paschmann, Max-Plank-Institut für extraterrestrische Physik, D-8046 Garching, Germany.

M. G. Kivelson and R. J. Walker, Institute of Geophysics and Planetary Physics, University of California, Los Angeles, CA 90024–1567.

H. Lühr, Institut für Geophysik und Meteorologie, Technische Universität Braunschweig, Mendelssohnstr. 3, D-3300 Braunschweig, Germany.

(Received March 11, 1991;
revised October 18, 1991;
accepted October 18, 1991.)